Depth-dependent static shielding of an impurity by a quantum plasma in a magnetic field

G. Gumbs and D. J. W. Geldart
Department of Physics, Dalhousie University, Halifax, Nova Scotia, Canada B3H 3J5
(Received 24 February 1983; revised manuscript received 8 November 1983)

The static shielding of a charged impurity embedded in a quantum plasma is studied with the use of linear-response theory. The required response function is calculated in the random-phase approximation with a uniform magnetic field applied in a direction perpendicular to the surface. The surface is assumed to be an infinite potential barrier. When quantum-interference effects between incident and reflected electrons scattered off the surface are ignored, an analog of the Debye-Thomas-Fermi shielding law for a semi-infinite plasma is derived when all electrons with the same spin are in the lowest Landau level. In the quantum strong-field limit, the induced electron number density is calculated numerically. The results, which exhibit Friedel-Kohn oscillations, are analyzed when the depth of the impurity below the surface is varied. It is suggested that these effects might be studied experimentally by conversion electron Mössbauer spectroscopy in appropriate materials.

I. INTRODUCTION

The static shielding of a charged impurity by a quantum plasma has been a subject of considerable interest. The problem has been divided into two areas of consideration. One is the shielding of an impurity in an infinite plasma, and the other is concerned with the effect which a surface has on the induced potential and screening charge around an impurity. However, as has been shown in non-self-consistent Hartree single-particle theory by Horing,[1,2] Rensink,[3] and Glasser[4,5] for a bulk plasma at zero temperature ($T=0$) in the presence of an external magnetic field, the shielding is spatially anisotropic. In addition, the Friedel-Kohn oscillatory behavior is significantly modified by high magnetic fields. It is the purpose of this paper to study the combined effect of Landau quantization and a surface in determining the static shielding law.

Our understanding of the static shielding of a point charge in an infinite plasma, in the absence of a magnetic field, is based on work of Friedel[6] and of Langer and Vosko.[7] The result of Langer and Vosko[7] for the induced charge density and screened potential at $T=0$ exhibits long-range oscillations with a radial wavelength π/k_F and an envelope proportional to r^{-3}, where k_F is the Fermi wave number and r is the distance from the impurity. The Thomas-Fermi approximation gives an exponential at large distances with the charge and effective potential confined to within a distance of the order of the Debye screening length. The corresponding problem for a semi-infinite plasma in the absence of a magnetic field has been studied by Equiluz[8] and others.

The result for the Debye-Thomas-Fermi (DTF) static shielding potential for an impurity in an infinite plasma, in the presence of a magnetic field, was first derived by Horing,[9] in the random-phase approximation (RPA). It was shown by Horing that the effective Debye length depends on the angle between the direction of the magnetic field and the position vector from the impurity. When all electrons with the same spin are in the lowest Landau level, it was shown that the Friedel-Kohn oscillatory behavior is modified by an exponential factor which damps the oscillations.

Beck, Celli, Lo Vecchio, and Magnaterra[10] have calculated the modification of the induced potential and charge density due to a surface, in the absence of a magnetic field. As a model for the surface, an infinite-barrier model (IBM) was used. Linear-response theory was assumed for the interaction between the impurity and conduction electrons in a uniform positive jellium background, and the response function was calculated in the RPA. It has been shown by Beck *et al.*[10] for the classical infinite-barrier model (CIBM), where quantum interference between incident and reflected electrons scattered off the surface is ignored, that the DTF static shielding law is given in terms of modified Bessel functions as well as exponential terms. The exponential terms are the long-wavelength shielding contribution for a bulk plasma. For both the CIBM and IBM, the shielded potential exhibits Friedel-Kohn oscillations. We note that Gadzuk[11] has also calculated some effects due to static shielding of an impurity by a quantum plasma with a surface in the absence of a magnetic field. However, Gadzuk's results do not take into account the shielding due to a surface charge distribution. That is, the electron-gas dispersion is not adequately included in the calculation. In this work, we generalize the above results by including the effects of an applied magnetic field.

In Sec. II we derive expressions for the shielded potential and charge density induced by an impurity which is embedded near the surface of a plasma of *finite thickness*. A uniform magnetic field is applied in a direction perpendicular to the surface. The linear-response formalism is used and the response function is calculated in the RPA. The electron eigenstates used are those appropriate to a jellium model with planar boundaries simulated by infinite potential barriers. Combining Poisson's equation with the linear-response equation, we obtain the dispersion relation for the collective modes of a *film*. The dispersion relation reduces to the result obtained by Gumbs and Griffin[12] for the half-space, when the thickness of the film is allowed to become infinite (in Ref. 12, this result was derived for an *external* charge).

In Sec. III, a numerical evaluation of the electron number density induced by an impurity in the surface region is carried out for the CIBM. Within this model, the total induced electron number density is compared with the contribution due to the surface of a semi-infinite plasma. The calculations are done in the absence of a magnetic field as well as in the quantum strong-field limit. For an impurity located at the surface of the plasma, the effect of a magnetic field in the quantum strong-field limit is to *reduce* the magnitude of the induced density on the surface by as much as 70%. The contribution to the induced electron number density due to the surface is itself reduced by as much as 75% in the quantum strong-field limit. This means that the effect of extremely high magnetic fields is to produce significant quantitative changes in the static shielding of a source. Calculations are also carried out to analyze the corresponding effects due to an impurity at varying distances from the surface. This method of calculation (RPA) treats plasmon dispersion satisfactorily. That is, the induced electron number density and the shielded potential are both given in terms of the density-response properties for excitations within a bounded plasma. This means that in the case of dynamical shielding the model response function has poles which correspond to the active plasmon resonances (bulk and surface). The formalism treats dynamical and static (time-averaged) shielding within the same approximations, with the latter being obtained by setting the frequency variable equal to zero.

In Sec. IV the DTF static shielding law for an impurity embedded near the surface of a semi-infinite plasma in an external magnetic field is obtained for the CIBM. In Sec. V we suggest an experiment which should verify these results. This experiment involves resolving the energies of backscattered electrons from the surface region of a Mössbauer absorber. By energy-resolving the flux of electrons, the spectra will be weighted towards a particular depth. This technique is referred to as depth-selective conversion-electron Mössbauer spectroscopy (DCEMS). The use of DCEMS in examining the depth dependence of the static shielding induced by a distribution of impurities should also be feasible in the presence of an external magnetic field (distinct from that used for energy resolution of emitted electrons), which could be used with some advantage in further probing the information provided by the backscattered electrons.

Surface impurity effects are of interest in a wide variety of situations. In particular, the adsorption of ions on metallic surfaces and their effects on corrosion, as well as the polarization produced in the surface region of a layered sample, have been a subject of much discussion.

These problems are of basic importance, but it is extremely difficult to treat rigorously the combination of effects due to the surface, the magnetic field, and the dynamical screening due to the Coulomb interaction between the impurity, which is taken as a point charge, and the plasma. To our knowledge, this is the first work where all of these effects have been simultaneously taken into account, albeit with simple approximations, and we hope that the results, which exhibit a quite marked dependence on the applied magnetic field, will stimulate further work with more sophisticated and extensive analysis.

II. INFINITE-BARRIER MODEL

In this section we calculate the potential and charge density induced by an impurity with charge Ze embedded in a bounded plasma. We extend the method of solution of the RPA equation for the response function of Beck *et al.*[10] to a film in the presence of a uniform magnetic field perpendicular to the surface. The film is bounded by infinite potential barriers at $z=0$ and L, but is unbounded in the $\vec{r}_{\parallel}$ plane (parallel to the surfaces). The point charge is inserted at $(0,0,z_0)$ *within* the otherwise uniform plasma, and the magnetic field of strength H_0 is in the z direction.

The general, frequency-dependent, induced charge density is, in linear-response theory, related to the total potential V by the equation

$$\rho(\vec{r},\omega)=\sum_{i,i'}\int d\vec{r}\,'\frac{f_0(E_i)-f_0(E_{i'})}{\hbar\omega+E_i-E_{i'}}\times\phi_i(\vec{r})\phi_{i'}^*(\vec{r})\phi_i^*(\vec{r}\,')\phi_{i'}(\vec{r}\,')V(\vec{r}\,',\omega)\ . \tag{2.1}$$

Here, $\phi_i(\vec{r})$ is an electron eigenstate of energy E_i, and $f_0(E_i)$ is the Fermi distribution function. For the infinite-barrier model (IBM), where the single-particle potential within the plasma is assumed uniform in the absence of the inserted charge, a complete set of unperturbed eigenstates is given by

$$\phi_{k_y,k_z,n}(\vec{r})=\left[\frac{2}{LA^{1/2}}\right]^{1/2}\xi_n(x-x_0(k_y))e^{ik_yy}\times\sin(k_zz)\ , \tag{2.2}$$

where the ξ_n are normalized harmonic-oscillator wave functions involving Hermite polynomials, with the cyclotron orbit centered at

$$x_0(k_y)\equiv-\frac{\hbar k_y}{m^*\omega_c},\quad \omega_c\equiv\frac{eH_0}{m^*c}\ . \tag{2.3}$$

Periodic boundary conditions have been imposed in the $\vec{r}_{\parallel}$ plane, and we take A to be the area of each plane slab face. The k_z wave number in Eq. (2.2) is restricted to $m\pi/L$ with $m=1,2,3,\ldots$ in order to ensure that the wave functions vanish at the surfaces $z=0$ and L. The scalar effective mass of an electron is m^* and the energy eigenvalues are

$$E(k_y,k_z,n)=\frac{\hbar^2k_z^2}{2m^*}+(n+\tfrac{1}{2})\hbar\omega_c\ , \tag{2.4}$$

with the Landau levels labeled by $n=0,1,2,\ldots$.

It is convenient to define a symmetric charge density by

$$\rho_s(\vec{q},\omega)=2\int d\vec{r}_{\parallel}\int_0^L dz\, e^{-i\vec{q}_{\parallel}\cdot\vec{r}_{\parallel}}\cos(q_z z)\rho(\vec{r},\omega)\ , \tag{2.5}$$

where $\vec{q}=(\vec{q}_{\parallel},q_z)$ with $q_z=0,\pm\pi/L,\pm 2\pi/L,\ldots$. Substituting the eigenfunctions (2.2) into Eq. (2.1) and then making use of the result for $\rho(\vec{r},\omega)$ in Eq. (2.5), we obtain

$$\rho_s(\vec{q},\omega)=\left[\frac{2}{LA^{1/2}}\right]\sum_{k_z n}\sum_{k_z' n'}\frac{f_0(E(k_z n))-f_0(E(k_z' n'))}{\hbar\omega-[E(k_z' n')-E(k_z n)]}\sum_{k_y k_y'}R(k_z,k_z';q_z)B(n,k_y;n',k_y';q_x)\delta_{q_y,k_y-k_y'}$$
$$\times\int_0^L dz'\sin(k_z' z')\sin(k_z z')\int dy' e^{-i(k_y-k_y')y'}$$
$$\times\int dx'\xi_n(x'-x_0(k_y))\xi_{n'}(x'-x_0(k_y'))V(\vec{r}\,',\omega)\ . \tag{2.6}$$

Here,

$$R(k_z,k_z';q_z)\equiv\frac{4}{L}\int_0^L dz\cos(q_z z)\sin(k_z z)\sin(k_z' z)\ , \tag{2.7}$$

$$B(n,k_y;n',k_y';q_x)\equiv\int dx\, e^{-iq_x x}\xi_n(x-x_0(k_y))\xi_{n'}(x-x_0(k_y'))$$
$$=e^{-iq_x x_0(k_y)}B_{nn'}(q_x,k_y-k_y')\ , \tag{2.8a}$$

with

$$B_{nn'}(q_x,q_y)\equiv\int dx\, e^{-iq_x x}\xi_n(x)\xi_{n'}(x+x_0(q_y))\ . \tag{2.8b}$$

Expanding $V(\vec{r},\omega)$ in terms of its k_x Fourier components, we have

$$\delta_{q_y,k_y-k_y'}\int dx'\xi_n(x'-x_0(k_y))\xi_{n'}(x'-x_0(k_y'))V(\vec{r}\,',\omega)=\frac{1}{A^{1/2}}\sum_{k_x}e^{ik_x x_0(k_y)}V(k_x,y',z')B_{nn'}^{*}(k_x,q_y)\delta_{q_y,k_y-k_y'}\ . \tag{2.9}$$

Therefore, making use of the results in Eqs. (2.8) and (2.9) in Eq. (2.6), we rewrite $\rho_s(\vec{q},\omega)$ as

$$\rho_s(\vec{q},\omega)=\frac{1}{2}\left[\frac{1}{LA}\right]\sum_{k_y}\sum_{k_z n}\sum_{k_z' n'}\frac{f_0(E(k_z n))-f_0(E(k_z' n'))}{\hbar\omega-[E(k_z' n')-E(k_z n)]}C_{nn'}(q_{\parallel})R(k_z,k_z';q_z)\int_0^L dz'\sin(k_z z')\sin(k_z' z')V(\vec{q}_{\parallel},z')\ , \tag{2.10}$$

where we have *now* extended the sums over k_z and k_z' in Eq. (2.10) to *all* multiples of π/L as well as zero since the $k_z,k_z'=0$ terms make no contribution to the sum. We also have

$$C_{nn'}(q_{\parallel})\equiv|B_{nn'}(q_x,q_y)|^2 \tag{2.11a}$$
$$=\frac{n!}{n'!}e^{-s}s^{n'-n}[L_n^{n'-n}(s)]^2\ , \tag{2.11b}$$

where $s\equiv\hbar q_{\parallel}^2/2m^*\omega_c$ and $L_n^{n'-n}$ is a Laguerre polynomial. The form for $C_{nn'}(q_{\parallel})$ in Eq. (2.11b) is due to Horing.[1]

Defining a symmetric potential $V_s(\vec{q},\omega)$ by

$$V_s(\vec{q},\omega)=2\int d\vec{r}_{\parallel}\int_0^L dz\, e^{-i\vec{q}_{\parallel}\cdot\vec{r}_{\parallel}}\cos(q_z z)V(\vec{r},\omega)\ , \tag{2.12}$$

it is possible to straightforwardly show that Eq. (2.10) may be rewritten as

$$\rho_s(\vec{q},\omega)=\chi^0(\vec{q},\omega)V_s(\vec{q},\omega)-\frac{1}{L}\sum_{q_z'}{}'S\left[\frac{q_z'-q_z}{2},\frac{q_z'+q_z}{2};q_{\parallel},\omega\right]V_s(q_z';q_{\parallel},\omega)\ , \tag{2.13}$$

where the prime on the summation in the second term of Eq. (2.13) means that the q_z''s summed over must have the same symmetry as q_z. $\chi^0(\vec{q},\omega)$ is the single-particle density-response function in the presence of a magnetic field in the z direction and is given by

$$\chi^0(\vec{q},\omega)=\frac{1}{2L}\sum_{k_z}S(k_z,k_z+q_z;q_{\parallel},\omega)\ , \tag{2.14}$$

where

$$S(k_z,k_z';q_{||},\omega)=\frac{1}{A}\sum_{k_y}\sum_{nn'}\frac{f_0(E(k_z,n))-f_0(E(k_z',n'))}{\hbar\omega-[E(k_z',n')-E(k_z,n)]}C_{nn'}(q_{||}) . \tag{2.15}$$

The potential and charge density are related by Poisson's equation,

$$V(z;q_{||},\omega)=(2\pi e/q_{||})\left[Ze\,e^{-q_{||}|z-z_0|}+\int_0^L dz'e^{-q_{||}|z-z'|}\rho(z';q_{||},\omega)\right] . \tag{2.16}$$

Therefore, $V_s(q,\omega)$ is given by

$$V_s(\vec{q},\omega)=\frac{4\pi e}{q^2}[2Ze\cos(q_zz_0)+\sigma(q_{||},\omega)+\rho_s(\vec{q},\omega)] , \tag{2.17}$$

which is a function of q_z and $q_{||}$ separately, with $q^2=q_z^2+q_{||}^2$. $\sigma(q_{||},\omega)$, which plays the role of a frequency-dependent surface charge density for the film, is given by

$$\begin{aligned}\sigma(q_{||},\omega)=&-Ze\,e^{-q_{||}L/2}[e^{-q_{||}(z_0-L/2)}-(-1)^m e^{q_{||}(z_0-L/2)}]\\&-e^{-q_{||}L/2}\int_0^L dz'\rho(z';q_{||},\omega)[e^{-q_{||}(z'-L/2)}+(-1)^m e^{q_{||}(z'-L/2)}] ,\end{aligned} \tag{2.18}$$

where m is the integer multiplying π/L for the wave number q_z in Eq. (2.17). Note that $\sigma(q_{||},\omega)$ of Eq. (2.17) is dependent on m (either even or odd). This should be remembered in the following derivation. We have

$$\frac{q_{||}}{L}\sum_{q_z}{}'\frac{\rho_s(q_z;q_{||},\omega)}{q_z^2+q_{||}^2}=\frac{1}{\sinh(q_{||}L/2)}\int_0^L dz\,\rho(z;q_{||},\omega)\cosh[q_{||}(z-L/2)] \tag{2.19a}$$

if the sum on the left-hand side of Eq. (2.19a) is over *even* multiples of π/L, and

$$\frac{q_{||}}{L}\sum_{q_z}{}'\frac{\rho_s(q_z;q_{||},\omega)}{q_z^2+q_{||}^2}=-\frac{1}{\cosh(q_{||}L/2)}\int_0^L dz\,\rho(z;q_{||},\omega)\sinh[q_{||}(z-L/2)] \tag{2.19b}$$

for a sum on q_z over *odd* multiples of π/L. Therefore, making use of the results of Eq. (2.19) in Eq. (2.18), we obtain

$$\sigma(q_{||},\omega)=-Ze[e^{-q_{||}z_0}-(-1)^m e^{-q_{||}(L-z_0)}]-[1-(-1)^m e^{-q_{||}L}]\frac{q_{||}}{L}\sum_{q_z}{}'\frac{\rho_s(q_z;q_{||},\omega)}{q_z^2+q_{||}^2} . \tag{2.20}$$

We introduce a function $\nu(\vec{q},\omega)$ in terms of the charge densities $\rho_s(\vec{q},\omega)$ and $\sigma(q_{||},\omega)$ by

$$\rho_s(\vec{q},\omega)=\sigma(q_{||},\omega)[\nu_0(\vec{q},\omega)-1]+2Ze[\nu(\vec{q},\omega)-\cos(q_zz_0)] , \tag{2.21}$$

where ν depends on the value of z_0, and ν_0 is the value of ν for $z_0=0$. We can straightforwardly express $\sigma(q_{||},\omega)$ of Eq. (2.20) in terms of ν. We have

$$\sigma(q_{||},\omega)=4Ze\left[\frac{(-1)^m e^{-q_{||}(L-z_0)}}{1-(-1)^m e^{-q_{||}L}}-\frac{q_{||}}{L}\sum_{q_z}{}'\frac{\nu(\vec{q},\omega)}{q_z^2+q_{||}^2}\right][1+R(q_{||},\omega)]^{-1} , \tag{2.22}$$

where

$$R(q_{||},\omega)=\frac{2q_{||}}{L}\sum_{q_z}{}'\frac{\nu_0(q_z;q_{||},\omega)}{q_z^2+q_{||}^2} . \tag{2.23}$$

The function $\nu(q,\omega)$ is determined from a set of coupled equations which are obtained by substituting Eq. (2.17) for $V_s(\vec{q},\omega)$ and Eq. (2.21) for $\rho_s(\vec{q},\omega)$ into Eq. (2.13). A short calculation gives

$$\nu(\vec{q},\omega)=\frac{1}{\epsilon(\vec{q},\omega)}\left[\cos(q_zz_0)-\frac{1}{L}\sum_{q_z'}{}'S\left[\frac{q_z'-q_z}{2},\frac{q_z'+q_z}{2};q_{||},\omega\right]v(q_z',q_{||})\nu(\vec{q},\omega)\right] , \tag{2.24}$$

where

$$\epsilon(\vec{q},\omega)\equiv 1-v(q)\chi^0(\vec{q},\omega) , \tag{2.25}$$

with $v(q)\equiv 4\pi e^2/(q_z^2+q_{||}^2)$ equal to the Fourier transform of the Coulomb potential. The collective excitations correspond to the solutions for which the denominator on the right-hand side of Eq. (2.22) vanishes, i.e.,

$$1+R(q_{||},\omega)=0 . \tag{2.26}$$

We note that the dispersion relation reduces to the half-space result derived previously,[12] when the limit $L\to\infty$ is taken. It should be observed that the sums on wave number for the full IBM are restricted to even or odd multiples of π/L, just as in the CIBM.

Multiplying both sides of Eq. (2.24) by $\epsilon(q,\omega)$ and then summing over q_z's which have the same parity as the q_z''s in the sum on the right-hand side of the equation, we obtain

$$\sum_{q_z}{}'[\nu(q_z;q_{||},\omega)-\cos(q_z z_0)]=0\ . \tag{2.27}$$

Therefore, from Eqs. (2.21) and (2.27), we have

$$\sum_{q_z}{}'\rho_s(q_z;q_{||},\omega)=0\ . \tag{2.28}$$

Setting $z=0$ and $z=L$, in turn, into the inverse of Eq. (2.5), and making use of the result in Eq. (2.28), we conclude that

$$\rho(z=0;q_{||},\omega)=0\ , \tag{2.29a}$$

$$\rho(z=L;q_{||},\omega)=0\ , \tag{2.29b}$$

i.e., the charge density vanishes at both boundaries, a result which is consistent with the IBM.

Substituting Eq. (2.17) into the inverse of Eq. (2.12) and then making use of Eq. (2.21), we obtain the total potential $V(\vec{r},\omega)$ within the film, $0\le z\le L$,

$$V(\vec{r},\omega)=\frac{1}{2L}\sum_{q_z}\int\frac{d\vec{q}_{||}}{(2\pi)^2}e^{i\vec{q}_{||}\cdot\vec{r}_{||}}\cos(q_z z)\frac{4\pi e}{q_z^2+q_{||}^2}[2Ze\nu(\vec{q},\omega)+\sigma(q_{||},\omega)\nu_0(\vec{q},\omega)]\ , \tag{2.30}$$

and the induced charge density there is

$$\rho(\vec{r},\omega)=\frac{1}{2L}\sum_{q_z}\int\frac{d\vec{q}_{||}}{(2\pi)^2}e^{i\vec{q}_{||}\cdot\vec{r}_{||}}\cos(q_z z)\{\sigma(q_{||},\omega)[\nu_0(\vec{q},\omega)-1]+2Ze[\nu(\vec{q},\omega)-\cos(q_z z_0)]\}\ . \tag{2.31}$$

We have thus obtained results for the linear shielding of an impurity within a film. Within this formalism, the set of coupled equations (2.24) has to be solved for $\nu(\vec{q},\omega)$. However, when surface-induced quantum-interference effects are neglected, $\nu(\vec{q},\omega)$ is given by the first term on the right-hand side of Eq. (2.24). Explicit results for this model are given in the next two sections.

III. CLASSICAL INFINITE-BARRIER MODEL

In the classical infinite-barrier model (CIBM), $\nu(\vec{q},\omega)$ of Eq. (2.24) is given by

$$\nu(\vec{q},\omega)=\frac{\cos(q_z z_0)}{\epsilon(\vec{q},\omega)}\ , \tag{3.1}$$

and $\nu_0(\vec{q},\omega)$ is equal to the inverse dielectric function. For this model, Eq. (3.1) is valid at arbitrary temperature and for arbitrary magnetic field strength, where the latter takes account of Landau quantization. Thus in the CIBM, we obtain, from Eqs. (2.30) and (2.31),

$$V(\vec{r},\omega)=\frac{1}{2L}\sum_{q_z}\int\frac{d\vec{q}_{||}}{(2\pi)^2}e^{i\vec{q}_{||}\cdot\vec{r}_{||}}\cos(q_z z)\frac{4\pi e}{q_z^2+q_{||}^2}\frac{2Ze\cos(q_z z_0)+\sigma(q_{||},\omega)}{\epsilon(q_z;q_{||},\omega)}\ , \tag{3.2a}$$

$$\rho(\vec{r},\omega)=\frac{1}{2L}\sum_{q_z}\int\frac{d\vec{q}_{||}}{(2\pi)^2}e^{i\vec{q}_{||}\cdot\vec{r}_{||}}\cos(q_z z)[2Ze\cos(q_z z_0)+\sigma(q_{||},\omega)]\left[\frac{1}{\epsilon(q_z;q_{||},\omega)}-1\right]\ , \tag{3.2b}$$

where the surface charge density defined in Eq. (2.22) is given by

$$\sigma(q_{||},\omega)=\frac{4Ze}{D(q_{||},\omega)}\left[\frac{(-1)^m e^{-q_{||}(L-z_0)}}{1-(-1)^m e^{-q_{||}L}}-\frac{q_{||}}{L}\sum_{q_z}{}'\frac{\cos(q_z z_0)}{(q_z^2+q_{||}^2)\epsilon(q_z;q_{||},\omega)}\right]\ . \tag{3.3}$$

In Eq. (3.3), $D(q_{||},\omega)$ is the *surface* dispersion formula defined by

$$D(q_{||},\omega)\equiv 1+\frac{2q_{||}}{L}\sum_{q_z}{}'\frac{1}{(q_z^2+q_{||}^2)\epsilon(q_z;q_{||},\omega)}\ , \tag{3.4}$$

the zeros of which give the normal modes of the film.[12–14]

In the half-space limit ($L\to\infty$), the real part of the static dielectric function at zero temperature and arbitrary magnetic field strength is given by

$$\epsilon(q,\omega=0)=1+v(q)\frac{2m^{*2}\omega_c}{(2\pi)^2\hbar^3|q_z|}\sum_{nn'}\eta_+(\mu-(n+\tfrac{1}{2})\hbar\omega_c)C_{nn'}(q_{||})\ln\left|\frac{\hbar(\frac{1}{2}q_z^2+k_F^{(n)}|q_z|)/m^*+(n'-n)\omega_c}{\hbar(\frac{1}{2}q_z^2-k_F^{(n)}|q_z|)/m^*+(n'-n)\omega_c}\right|\ , \tag{3.5}$$

where the matrix element $C_{nn'}(q_{||})$ is defined in Eq. (2.11),

$$k_F^{(n)} \equiv \left[\frac{2m^*}{\hbar^2}[\mu-(n+\tfrac{1}{2})\hbar\omega_c] \right]^{1/2} , \tag{3.6}$$

and μ is the chemical potential. The step function η_+ sets an upper limit on the sum over occupied states. For magnetic fields so strong that all electrons are in the lowest Landau level, i.e., the chemical potential is comparable with the energy scale of quantized cyclotron motion, only the $n=0$ term contributes to the sum in Eq. (3.5). Equation (2.11) gives $C_{n=0,n'}(q_{||})=e^{-s}s^{n'}/n'!$. Substituting this result in Eq. (3.5), we obtain

$$\epsilon(\vec{q},\omega=0)=1+\frac{k_D^2 k_F}{q^2|q_z|}e^{-q_{||}^2/p_H^2}\left[\ln\left|\frac{|q_z|+2k_F^{(0)}}{|q_z|-2k_F^{(0)}}\right| + \sum_{n'=1}^{\infty}\frac{1}{n'!}\left[\frac{q_{||}}{p_H}\right]^{2n'} \ln\left|\frac{\hbar(\frac{1}{2}q_z^2+k_F^{(0)}|q_z|)/m^*+n'\omega_c}{\hbar(\frac{1}{2}q_z^2-k_F^{(0)}|q_z|)/m^*+n'\omega_c}\right| \right] , \tag{3.7}$$

where $k_D^2 k_F \equiv (m^*\omega_p^2/\hbar\sqrt{\mu}\ (m^*/2)^{1/2}$ and $p_H \equiv (2m^*\omega_c/\hbar)^{1/2}$. The plasma frequency is given by $\omega_p^2=4\pi\bar{n}e^2/m^*$ where, in the quantum strong-field limit, the electron density is $\bar{n}=(m^{*3}\omega_c^2\mu/2)^{1/2}/\pi^2\hbar^2$. k_F is defined by $k_F=(2m^*\mu/\hbar^2)^{1/2}$.

Substituting Eq. (3.5) into Eq. (3.2), with $L=\infty$ and $\omega=0$, we obtain the static shielded potential for a semi-infinite plasma in the CIBM. We write the result as

$$V(\vec{r},\omega=0)=V_1(\vec{r})+V_2(\vec{r}) , \tag{3.8}$$

where

$$V_1(\vec{r})=\frac{4\pi Ze^2}{(2\pi)^3}\int d\vec{q}\, e^{i\vec{q}_{||}\cdot\vec{r}_{||}}\{\cos(q_z|z-z_0|)+\cos[q_z(z+z_0)]\}\frac{1}{(q_z^2+q_{||}^2)\epsilon(q_z;q_{||},\omega=0)} , \tag{3.9}$$

$$V_2(\vec{r})=-\frac{16\pi Ze^2}{(2\pi)^3}\int dq\, e^{i\vec{q}_{||}\cdot\vec{r}_{||}}\cos(q_z z)\frac{N(q_{||})}{D(q_{||},\omega=0)}\frac{1}{(q_z^2+q_{||}^2)\epsilon(q_z;q_{||},\omega=0)} , \tag{3.10}$$

where $N(q_{||})$ is the integral for the surface charge density $\sigma(q_{||},\omega=0)$ for the half-space geometry and is given by

$$N(q_{||})=\frac{q_{||}}{2\pi}\int_{-\infty}^{\infty} dq_z \cos(q_z z_0)\frac{1}{(q_z^2+q_{||}^2)\epsilon(q_z;q_{||},\omega=0)} . \tag{3.11}$$

Similarly, we have the static density distribution for a half-space in the CIBM. The result is, from Eq. (3.2),

$$\rho(\vec{r},\omega=0)=\rho_1(\vec{r})+\rho_2(\vec{r}) , \tag{3.12}$$

where

$$\rho_1(\vec{r})=\frac{Ze}{(2\pi)^3}\int d\vec{q}\, e^{i\vec{q}_{||}\cdot\vec{r}_{||}}\{\cos(q_z|z-z_0|)+\cos[q_z(z+z_0)]\}\left[\frac{1}{\epsilon(q_z;q_{||},\omega=0)}-1\right] , \tag{3.13}$$

$$\rho_2(\vec{r})=-\frac{4Ze}{(2\pi)^3}\int d\vec{q}\, e^{i\vec{q}_{||}\cdot\vec{r}_{||}}\cos(q_z z)\frac{N(q_{||})}{D(q_{||},\omega=0)}\left[\frac{1}{\epsilon(q_z;q_{||},\omega=0)}-1\right] . \tag{3.14}$$

Both $V_1(\vec{r})$ in Eq. (3.9) and $\rho_1(\vec{r})$ in Eq. (3.13) are contributions to *bulk* screening from the impurity and its image in the surface. On the other hand, $V_2(\vec{r})$ and $\rho_2(\vec{r})$, defined, respectively, in Eqs. (3.10) and (3.14), are due to *surface* collective effects.

In the non-self-consistent Hartree single-particle approximation, the screening contributions to the induced density, including collective modes, are not included. Thus, $\rho_2(\vec{r})$ arising from the surface modes is neglected and $\rho_1(\vec{r})$ is approximated by[15]

$$\rho_{\rm Hartree}(\vec{r})=Ze\int d\vec{r}\,'\chi^0(\vec{r},\vec{r}\,';\omega=0)v(\vec{r}\,') . \tag{3.15}$$

The induced electron number density has been calculated previously with the use of Eq. (3.15) in a case of a contact interaction, $v(\vec{r})=v_0\delta(\vec{r}-\vec{r}_0)$, and for the case of a shielded Coulomb potential,

$$v(\vec{r})=(Ze^2/|\vec{r}-\vec{r}_0|)\exp(-\kappa|\vec{r}-\vec{r}_0|) .$$

It is of interest to determine whether the parameters of these approximations can be adjusted so as to reproduce the RPA results reported here. This turns out not to be possible. For example, the contact interaction, having only one parameter, can be adjusted to reproduce the long-range Friedel oscillations, but the phase of these oscillations is not given correctly. The screened Coulomb potential has more flexibility and can be adjusted to reproduce the long-range oscillations, but then the behavior near the impurity is not so well described.

In examining the effect of a magnetic field on the induced electron number density in the RPA, we have computed $\rho(\vec{r})$ in the absence of a magnetic field as well as in the quantum high-field limit. The results are plotted in Figs. 1—3. The calculations for the high-field quantum limit are based on the results in Eq. (3.12) with the bulk dielectric function given by Eq. (3.7). For the calculations in the absence of a magnetic field, Eq. (3.12) was used with the bulk dielectric function in Eqs. (3.13) and (3.14) given by the well-known result for $\epsilon(\vec{q},\omega=0)$ involving the Lindhard function, in the absence of a magnetic field. The electron number density $\bar{n}$ is chosen to be 0.768×10^{17} cm^{-3} and the scalar effective mass of an electron is $m^*=0.01m_e=0.911\times10^{-29}$ g, which are appropriate for a semiconductor such as InSb. At zero temperature, the Fermi energy in the absence of a magnetic field is given by

$$\mu_0=\frac{\hbar^2\pi^2}{2m^*}\left[\frac{6\bar{n}}{\pi}\right]^{2/3} . \tag{3.16}$$

Thus with our choice of electron number density and effective mass for the electron, $\mu_0=0.105$ eV and $k_{Fn}\equiv(6\bar{n}\pi^2)^{1/3}=0.017$ Å^{-1}, it can be shown that in the high-field quantum limit, with one Landau energy level occupied the chemical potential, μ is given by[16]

$$\mu=\tfrac{1}{2}\hbar\omega_c+\frac{4}{9}\frac{\mu_0^3}{(\hbar\omega_c)^2} . \tag{3.17}$$

The magnetic field H_0 is chosen to be 200 kG. Thus $\hbar\omega_c=0.231$ eV, and from Eq. (3.17) we obtain the chemical potential $\mu=0.125$ eV. The quantum high-field limit ($\frac{1}{2}\hbar\omega_c\le\mu<\frac{3}{2}\hbar\omega_c$) is thus satisfied, i.e., all electrons are in the lowest Landau energy level.

In Fig. 1 we have plotted the total induced electron number density $\rho(\vec{r})$ and the contribution $\rho_2(\vec{r})$ associated with the surface dispersion formula, for the CIBM. An impurity is located at the surface of the plasma. The induced electron number density is plotted as a function of distance into the plasma along the polar axis perpendicular to the surface. For Figs. 1(a) and 1(b), the magnetic field $H_0=0$, whereas $H_0=200$ kG in Figs. 1(c) and 1(d). This magnetic field satisfies the quantum high-field limit for a degenerate plasma with all electrons in the lowest Landau energy level. The effect of the field is to significantly reduce the amplitude of the induced electron number density within a few Fermi wavelengths from the surface. The results in Fig. 1 also show that the long-range oscillatory behavior of the induced electron number density in the quantum high-field limit has a Friedel-Kohn–type "wiggle" in a direction parallel to the magnetic field. In Fig. 2 the total induced electron number density $\rho(\vec{r})$ due to an impurity on the polar axis at $z_0=2k_F^{-1}$ within the plasma is calculated. For Fig. 2(a) the magnetic field $H_0=0$. The magnetic field $H_0=200$ kG for Fig. 2(b). In Fig. 2, $\rho(\vec{r})$ is plotted for points $\vec{r}$ lying along the polar axis for a degenerated plasma. Comparing Fig. 1(a) with Fig. 2(a) and Fig. 1(c) with Fig. 2(b) we find that the value of the induced electron number density ρ at the source can be reduced by as much as 15% when the impurity is moved from a point on the surface to a point $z_0=2k_F^{-1}$ within the plasma. In the absence of an external magnetic field, ρ is shown as having Friedel-Kohn oscillations for values of $z\gtrsim z_0$. As the value of z_0 increases, numerical calculation shows that oscillations in ρ appear for $0\lesssim z\lesssim z_0$. In Fig. 3 we plot ρ in the direction perpendicular to the magnetic field for an impurity on the surface. Figure 3(a) shows that there are Friedel-Kohn oscillations in the total induced electron number density. A comparison of Fig. 3(b) with Fig. 1(d) shows how highly anisotropic the Friedel-Kohn oscillatory behavior is in the quantum strong-field limit.

It is clear from the above that the magnetic field dependence of the induced electron density around impurities, including the Friedel-Kohn quantum density oscillations, is very sensitive to variations in the applied magnetic field. Although these numerical results are based on simple treatments of the surface effects, in particular the CIBM, it is clearly to be expected that this sensitivity to the magnetic field will also be found in more precise treatments. There are also situations where the screening properties of the plasma are simplified by using long-wavelength approximations. This is discussed in the following section.

IV. DEBYE-THOMAS-FERMI STATIC SHIELDING LAW

Substituting the long-wavelength approximations for the matrix element $C_{nn'}(q_{\parallel})$ defined in Eq. (2.11), namely

$$C_{n\,n}(q_{\parallel})=1-(n+\tfrac{1}{2})\bar{q}_{\parallel}^2+O(q_{\parallel}^4) , \tag{4.1a}$$

$$C_{n\,n+1}(q_{\parallel})=\tfrac{1}{2}(n+1)\bar{q}_{\parallel}^2+O(q_{\parallel}^4) , \tag{4.1b}$$

$$C_{n\,n+m}(q_{\parallel})=O(q_{\parallel}^{2m}) , \tag{4.1c}$$

into Eq. (2.14) [here $\bar{q}_{\parallel}\equiv q_{\parallel}/(m^*\omega_c/\hbar)^{1/2}$], it is a simple matter to show that, for zero frequency,

$$\chi^0(\vec{q},\omega=0)\approx-\frac{\partial\bar{n}}{\partial\mu}+\frac{\hbar^2q_z^2}{4m^*}\frac{\partial^2\bar{n}}{\partial\mu^2}+\frac{q_{\parallel}^2}{m^2\omega_c^2}\left[\frac{\partial W}{\partial\mu}-\bar{n}\right] , \tag{4.2}$$

where

$$\bar{n}\equiv\frac{1}{2L}\sum_{k_z}\sum_{n}f_0(E(k_z,n)) , \tag{4.3}$$

$$W\equiv\frac{1}{2L}\sum_{k_z}\sum_{n}(n+\tfrac{1}{2})\hbar\omega_c f_0(E(k_z,n)) . \tag{4.4}$$

Here $\bar{n}$ is the number density per unit volume and W is the mean oscillator "potential energy." The results in Eqs. (4.1)–(4.4) are valid for arbitrary magnetic field strength and at arbitrary temperature.

In the limit of zero temperature, $\chi^0(\vec{q},\omega=0)$ of Eq. (4.2) contains sums of δ functions which cause the linear-response theory to become unreliable in the absence of broadening of the Landau energy levels. Whenever the chemical potential matches the energy of one of the Landau levels of finite slabs or quasi-two-dimensional electronic systems,[17,18] the above-mentioned limiting procedures are not well defined. For present applications, we restrict our attention to the static shielding of an impurity for the half-space geometry and the CIBM. In the limit $L\to\infty$, the sums over the q_z wave number are replaced by integrals. Substituting the long-wavelength result for $\chi^0(\vec{q},\omega=0)$ in Eq. (4.2) into Eq. (3.4), and then doing the q_z integration, we obtain

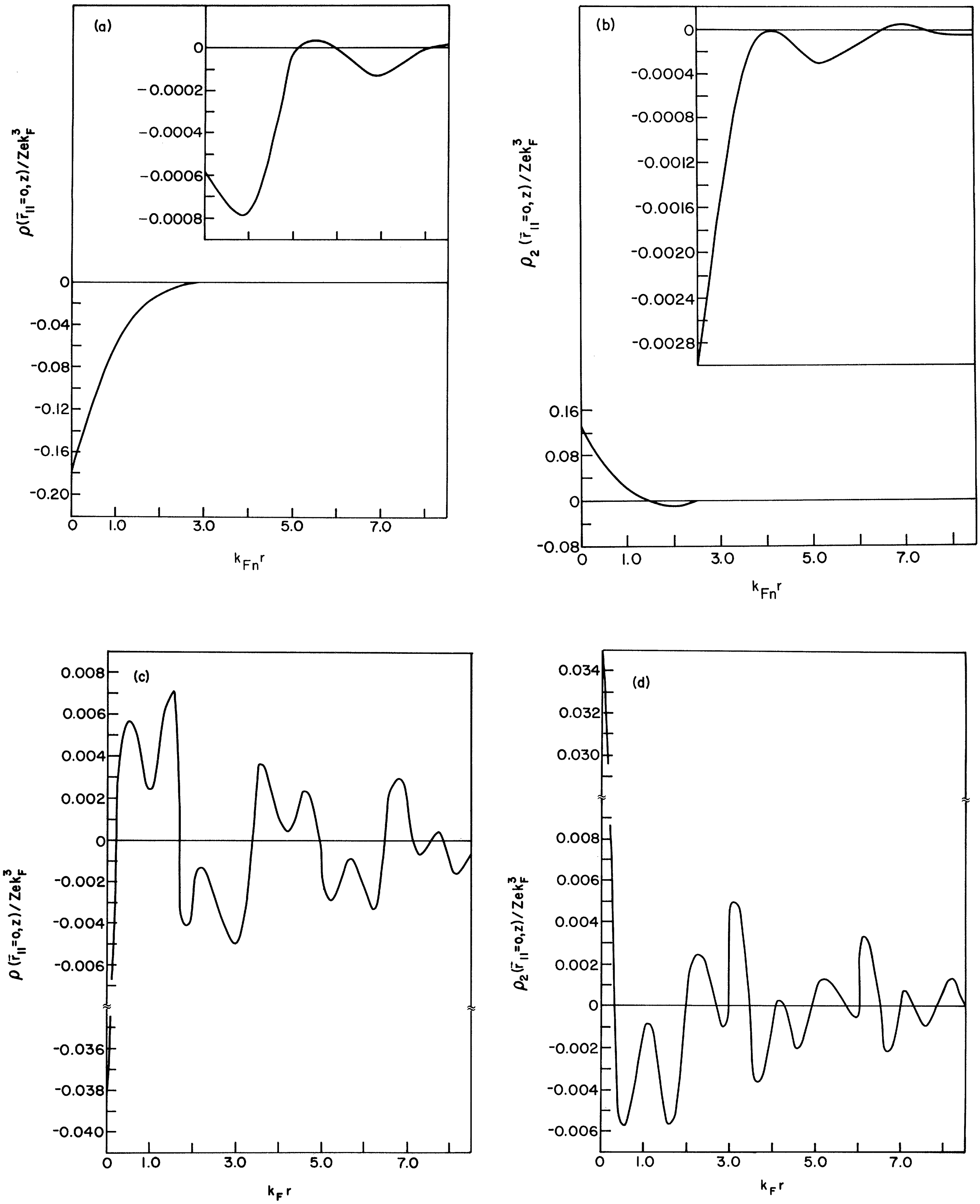

FIG. 1. This figure compares the total induced electron number density ρ and the contribution ρ_z due to the surface for the CIBM of a semi-infinite plasma. An impurity is located at the surface of the plasma and the induced density is plotted as a function of distance into the plasma measured from the impurity along the polar axis perpendicular to the surface. For (a) and (b) the magnetic field $H_0=0$, while $H_0=200$ kG for (c) and (d). The insets of (a) and (b) show the Friedel-Kohn oscillatory behavior and have the same scale for the spatial coordinate.

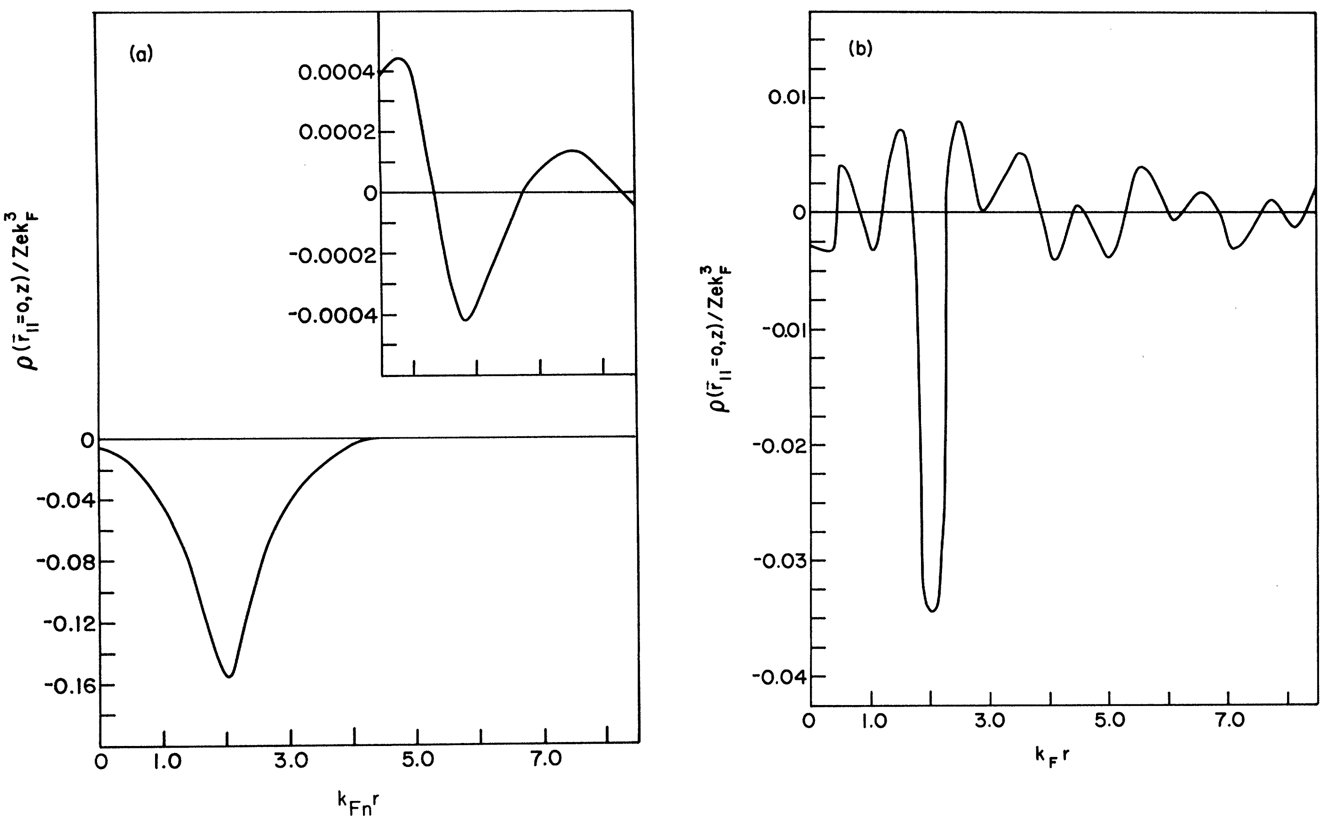

FIG. 2. Total induced electron number density for the CIBM of a semi-infinite plasma, along the polar z axis. An impurity is on the polar axis at $z_0=2k_F^{-1}$ within the plasma. For (a) the magnetic field $H_0=0$, while $H_0=200$ kG for (b). The inset of (a) shows the Friedel-Kohn oscillatory behavior.

$$D(q_{\parallel},\omega=0)=1+\frac{q_{\parallel}}{A(q_{\parallel})}\left[1-\frac{\pi e^2\hbar^2}{m^*}\frac{\partial^2\bar{n}}{\partial\mu^2}\right]^{-1}, \tag{4.5}$$

where

$$A(q_{\parallel})\equiv\left[\frac{4\pi e^2\dfrac{\partial\bar{n}}{\partial\mu}+\left[1-\dfrac{4\pi e^2}{m^*\omega_c^2}\left[\dfrac{\partial W}{\partial\mu}-\bar{n}\right]\right]q_{\parallel}^2}{1-\dfrac{\pi e^2\hbar^2}{m^*}\dfrac{\partial^2\bar{n}}{\partial\mu^2}}\right]^{1/2}. \tag{4.6}$$

With the use of Eq. (4.2) in Eq. (3.3), we obtain the static surface charge density for a half-space as

$$\sigma(q_{\parallel},\omega=0)=-2Ze\frac{q_{\parallel}\exp[-z_0A(q_{\parallel})]}{q_{\parallel}+\left[1-\dfrac{\pi e^2\hbar^2}{m^*}\dfrac{\partial^2\bar{n}}{\partial\mu^2}\right]A(q_{\parallel})}. \tag{4.7}$$

Substituting Eqs. (4.2), (4.5), and (4.7) into Eqs. (3.9) and (3.10), we obtain

$$V_1(\vec{r})=V_B(\vec{r}_+)+V_B(\vec{r}_-), \tag{4.8}$$

where

$$V_B(\vec{r}_\pm)=\frac{\dfrac{Ze^2}{r_\pm}\exp\left[-r_\pm\left\{\left[4\pi e^2\dfrac{\partial\bar{n}}{\partial\mu}\right]^{1/2}\Big/\left[1-\dfrac{4\pi e^2}{m^*\omega_c^2}\left[\dfrac{\partial W}{\partial\mu}-\bar{n}\right]\right]^{1/2}\right\}(1+\delta\cos^2\theta_\pm)^{1/2}\right]}{\eta(1+\delta\cos^2\theta_\pm)^{1/2}}, \tag{4.9}$$

$$\delta\equiv\frac{\dfrac{4\pi e^2}{m^*}\left[\dfrac{\hbar^2}{4}\dfrac{\partial^2\bar{n}}{\partial\mu^2}-\dfrac{1}{\omega_c^2}\left[\dfrac{\partial W}{\partial\mu}-\bar{n}\right]\right]}{1-\dfrac{\pi e^2\hbar^2}{m^*}\dfrac{\partial^2\bar{n}}{\partial\mu^2}}, \tag{4.10}$$

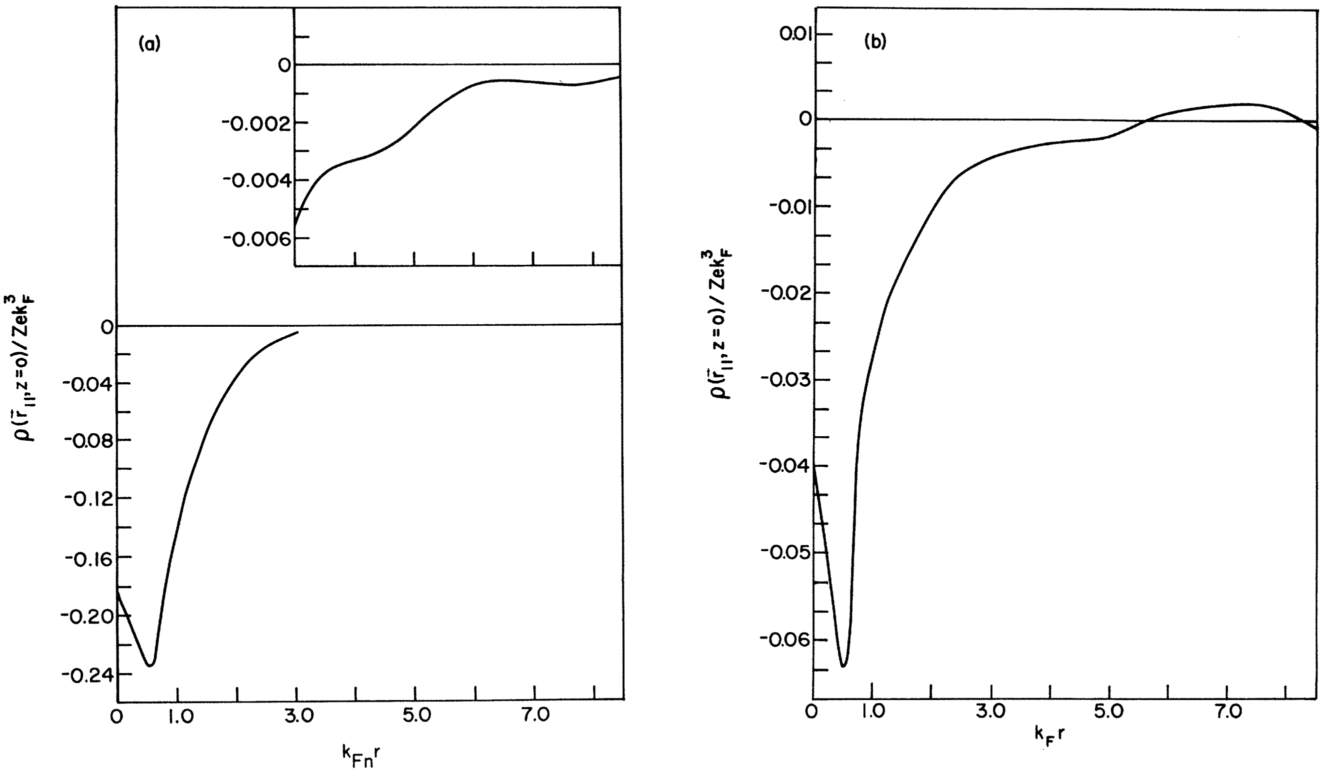

FIG. 3. Total induced electron number density along a line passing through an impurity at $z_0=0$, and parallel to the surface as a function of distance from the source. For (a) the magnetic field $H_0=0$, while $H_0=200$ kG for (b). The inset of (a) displays the Friedel-Kohn oscillations.

$$\eta \equiv \left[1-\frac{4\pi e^2}{m^*\omega_c^2}\left[\frac{\partial W}{\partial \mu}-\bar n\right]\right]^{1/2}\left[1-\frac{\pi e^2\hbar^2}{m^*}\frac{\partial^2 \bar n}{\partial \mu^2}\right]^{1/2} . \tag{4.11}$$

Here $\theta_\pm$ is the angle between the magnetic field and the spatial vector $\vec r_\pm=(\vec r_{\|},z\pm z_0)$. The contribution $V_2(\vec r)$ to the shielding is, in this approximation, given by

$$V_2(\vec r)=-\frac{-2Ze^2}{1-\frac{4\pi e^2}{m^*\omega_c^2}\left[\frac{\partial W}{\partial \mu}-\bar n\right]}\mathscr{I}(\eta;\vec r) , \tag{4.12}$$

where $\mathscr{I}(\eta;\vec r)$ is an integral defined by

$$\mathscr{I}(\eta;r)\equiv \int_0^\infty dk_{\|}k_{\|}^2 \exp\left[-(z'+z_0')\left[4\pi e^2\frac{\partial \bar n}{\partial \mu}+k_{\|}^2\right]^{1/2}\right]\frac{J_0(k_{\|}r_{\|}')}{\left[4\pi e^2\frac{\partial \bar n}{\partial \mu}+k_{\|}^2\right]^{1/2}}\frac{1}{k_{\|}+\eta\left[4\pi e^2\frac{\partial \bar n}{\partial \mu}+k_{\|}^2\right]^{1/2}} , \tag{4.13}$$

with

$$\begin{Bmatrix} z' \\ z_0' \end{Bmatrix}=\begin{Bmatrix} z \\ z_0 \end{Bmatrix}\left[1-\frac{\pi e^2\hbar^2}{m^*}\frac{\partial^2 \bar n}{\partial \mu^2}\right]^{-1/2} , \tag{4.14a}$$

$$r_{\|}'=r_{\|}\left[1-\frac{4\pi e^2}{m^*\omega_c^2}\left[\frac{\partial W}{\partial \mu}-\bar n\right]\right]^{-1/2} . \tag{4.14b}$$

$V_B(\vec r_-)$ and $V_B(\vec r_+)$ are, respectively, the DTF contributions to the potential from the impurity and its image in the surface. Thus $V_1(\vec r)$ is due to classical specular scattering, with the electronic properties described by the bulk response function. The role played by the surface collective excitations in shielding the impurity in the DTF approximation is given by Eq. (4.12).

The term $\partial\bar{n}/\partial\mu$ in Eq. (4.2) gives rise to quantum effects associated with the presence of a magnetic field. Additional quantum corrections are due to the q_z^2 and $q_{\parallel}^2$ terms.[9] If these quantum corrections are small, η in Eq. (4.11) is approximately unity. In this approximation, the integral $\mathscr{I}(\eta)$ in Eq. (4.13) can be done analytically. This is shown in the appendix using results of Gradshteyn and Ryzhik.[19] With the use of the results in the Appendix, we obtain, for $V_2(\vec{r})$,

$$V_2(\vec{r})=\frac{2Ze^2/\gamma^2\eta^2}{1-\dfrac{4\pi e^2}{m^*\omega_c^2}\left[\dfrac{\partial W}{\partial\mu}-\bar{n}\right]}\left[\left[\frac{\partial^2}{\partial\alpha^2}-\gamma^2\right][F^{(1)}(\alpha;\beta,\gamma)+\eta F^{(2)}(\alpha;\beta,\gamma)]\right.$$
$$\left.-\frac{1}{\gamma^2}\frac{\eta^2-1}{\eta^2}\left[\frac{\partial^2}{\partial\alpha^2}-\gamma^2\right]^2[F^{(1)}(\alpha;\beta,\gamma)-\eta F^{(2)}(\alpha;\beta,\gamma)]\right]. \tag{4.15}$$

The functions $F^{(1)}$ and $F^{(2)}$ are defined in Eqs. (A3) and (A4), respectively. For convenience of notation, the variables α, β, and γ appearing in Eq. (4.15) are defined to be

$$\alpha\equiv z'+z_0' , \tag{4.16a}$$

$$\beta\equiv r_{\parallel}' , \tag{4.16b}$$

$$\gamma\equiv\left[4\pi e^2\frac{\partial\bar{n}}{\partial\mu}\right]^{1/2} . \tag{4.16c}$$

Equations (4.8)—(4.16) thus give the analog of the DTF static shielding law for an impurity embedded near the surface of a semi-infinite quantum plasma. We emphasize that the result for $V_2(\vec{r})$ in Eq. (4.15) is based on the assumption that the quantum corrections to $\partial\bar{n}/\partial\mu$ in Eq. (4.2) are sufficiently small for one to take $\eta-1$ as a small parameter. From the results in Sec. II of Ref. 9, one determines the conditions under which the approximation $\eta\approx1$ is satisfied. For example, in the quantum strong-field limit, if both $\omega_p<\omega_c$ and $\mu/4\hbar\omega_c\lesssim1$ are satisfied, the result $\eta\approx1$ is obtained.[20]

The approximation for the frequency-dependent bulk dielectric function to order q^2 gives magnetoplasmon modes in the long-wavelength limit. Higher-order terms in $\epsilon(\vec{q},\omega)$ give "Bernstein"-type plasmon resonances[13] near each higher multiple of the cyclotron frequency $n\omega_c$ ($n\geq2$) for propagation nearly perpendicular to the magnetic field, and "quantum"-type plasmon resonances near each higher multiple of the cyclotron frequency $n\omega_c$ ($n\geq2$) for propagation off the perpendicular direction.[14,21] It has been demonstrated by Horing, Danz, and Glasser[22] that in the quantum strong-field limit, the contribution to the bulk correlation energy from both the "Bernstein"-type modes and the "quantum"-type plasmon resonances is small compared with the magnetoplasmon modes. Thus it is clear that the present calculation of long-range static shielding is consistent with the calculation of the bulk correlation energy, in the quantum strong-field limit.

V. CONCLUSION

It is known that the electrons emitted in the Mössbauer process of depth-selective conversion-electron Mössbauer spectroscopy (DCEMS) could be used to study the surface layers of a Mössbauer absorber.[23] Recently, depth-selective Mössbauer spectroscopy involving the detection of conversion electrons has been used to probe magnetic hyperfine interaction and isomer shift as a function of depth in iron films.[23] Thus we feel that a conversion-electron investigation would be a useful experiment to study the depth dependence of the static shielding in the presence of an externally applied magnetic field. The isomer shift for Sb is relatively large.[24] The small effective mass and low electron number density of InSb make it possible for the quantum strong-field limit to be achieved. Thus our predictions may be verifiable in an experimental study using DCEMS for InSb where high-magnetic-field conditions are favorable. Of course, InSb has a diamond-crystal lattice and the band structure has been determined.[25] The Fermi surface for this group—III-V compound is more like that of the group-IV element Ge, which also has a diamond lattice, rather than that of the free-electron spherical model. However, the free-electron-gas model is the simplest model to study the effect of applying a magnetic field and is sufficient to demonstrate that the effects are numerically very significant.

Several theories[26—28] have been used to derive expressions relating the observed Mössbauer signal to layer thickness in the absence of an external magnetic field. The results of Refs. 26—28 would have to be generalized to include a magnetic field should they by useful in the interpretation of a DCEMS experiment where an external magnetic field is applied. These experiments are expected to be difficult, but they would be very valuable. Finally, we emphasize again that the present calculations have been carried out within simple approximations, which nonetheless, allow simultaneous consideration of the surface effects, the perpendicular magnetic field, and dynamical screening. The resulting magnetic field dependence of the induced electron number density around impurities is found to be significant, and we hope that the present work will encourage further study.

APPENDIX: APPROXIMATE EVALUATION OF $\mathscr{I}(\eta)$

In this appendix, we evaluate the integral $\mathscr{I}(\eta)$ defined by Eq. (4.13) for a value of η approximately equal to unity. Rewriting Eq. (4.13), we have

$$\mathscr{I}(\eta)=\int_0^\infty dk_{\|}k_{\|}^2\exp[-(z'+z_0')(4\pi e^2\partial\bar{n}/\partial\mu+k_{\|}^2)^{1/2}]J_0(k_{\|}r_{\|}') \times\left[\eta-\frac{k_{\|}}{(4\pi e^2\partial\bar{n}/\partial\mu+k_{\|}^2)^{1/2}}\right]\frac{1}{(4\pi e^2\partial\bar{n}/\partial\mu)\eta^2+(\eta^2-1)k_{\|}^2} . \tag{A1}$$

Expanding the denominator in the last factor of Eq. (A1) in powers of η^2-1, we have

$$\mathscr{I}(\eta)\approx\frac{1}{(4\pi e^2\partial\bar{n}/\partial\mu)\eta^2}\int_0^\infty dk_{\|}\exp[-(z'+z_0')(4\pi e^2\partial\bar{n}/\partial\mu+k_{\|}^2)^{1/2}] \times J_0(k_{\|}r_{\|}')\left[\eta k_{\|}^2-\frac{k_{\|}^3}{(4\pi e^2\partial\bar{n}/\partial\mu+k_{\|}^2)^{1/2}}+\frac{\eta^2-1}{\eta^2}\frac{1}{4\pi e^2\partial\bar{n}/\partial\mu}\frac{k_{\|}^5}{(4\pi e^2\partial\bar{n}/\partial\mu+k_{\|}^2)^{1/2}} -\frac{\eta^2-1}{\eta^2}\frac{k_{\|}^4}{(4\pi e^2\partial\bar{n}/\partial\mu)}\right] . \tag{A2}$$

Each term in Eq. (A2) yields an integral whose evaluation we now discuss separately.

Making use of the results in 6.616(2) and 6.637(1) of Gradshteyn and Ryzhik,[19] we have

$$F^{(1)}(\alpha;\beta,\gamma)\equiv\int_0^\infty dx\,x\exp[-\alpha(\gamma^2+x^2)^{1/2}]\frac{J_0(\beta x)}{(\gamma^2+x^2)^{1/2}} =\frac{1}{(\alpha^2+\beta^2)^{1/2}}\exp[-\gamma(\alpha^2+\beta^2)^{1/2}] , \tag{A3}$$

$$F^{(2)}(\alpha;\beta,\gamma)=\int_0^\infty dx\exp[-\alpha(\gamma^2+x^2)^{1/2}]\frac{J_0(\beta x)}{(\gamma^2+x^2)^{1/2}} =I_0(\tfrac{1}{2}\gamma[(\alpha^2+\beta^2)^{1/2}-\alpha])K_0(\tfrac{1}{2}\gamma[(\alpha^2+\beta^2)^{1/2}+\alpha]) , \tag{A4}$$

where I_0 and K_0 are modified Bessel functions.

Treating α, β, and γ as independent variables, we find that

$$\int_0^\infty dx\,x^2\exp[-\alpha(\gamma^2+x^2)^{1/2}]J_0(\beta x)=\int_0^\infty dx(\gamma^2+x^2)\exp[-\alpha(\gamma^2+x^2)^{1/2}]J_0(\beta x) , -\gamma^2\int_0^\infty dx\exp[-\alpha(\gamma^2+x^2)^{1/2}]J_0(\beta x)=-\frac{\partial}{\partial\alpha}\left[\frac{\partial^2}{\partial\alpha^2}-\gamma^2\right]F^{(2)}(\alpha;\beta,\gamma) . \tag{A5}$$

This result gives the integral for the first term in Eq. (A2).

It is a simple matter to show that

$$\int_0^\infty dx\frac{x^3}{(\gamma^2+x^2)^{1/2}}\exp[-\alpha(\gamma^2+x^2)^{1/2}]J_0(\beta x)=\left[\frac{\partial^2}{\partial\alpha^2}-\gamma^2\right]F^{(1)}(\alpha;\beta,\gamma) , \tag{A6}$$

$$\int_0^\infty dx\frac{x^5}{(\gamma^2+x^2)^{1/2}}\exp[-\alpha(\gamma^2+x^2)^{1/2}]J_0(\beta x)=\left[\frac{\partial^4}{\partial\alpha^4}-2\alpha^2\frac{\partial^2}{\partial\alpha^2}+\gamma^4\right]F^{(2)}(\alpha;\beta,\gamma) , \tag{A7}$$

and

$$\int_0^\infty dx\,x^4\exp[-\alpha(\gamma^2+x^2)^{1/2}]J_0(\beta x)=\left[\frac{\partial^4}{\partial\alpha^4}-2\gamma^2\frac{\partial^2}{\partial\alpha^2}+\gamma^4\right]F^{(2)}(\alpha;\beta,\gamma) . \tag{A8}$$

With the use of the results of Eqs. (A6)—(A8), we obtain the integrals for the remaining terms in Eq. (A2), with α, β, and γ defined in Eq. (4.16). We have thus completely determined the integral $\mathscr{I}(\eta)$ and hence $V_2(\vec{r})$ of Eq. (4.12) to lowest order in η^2-1. $V_2(\vec{r})$, to this order, is given in Eq. (4.15), and higher-order corrections can also be calculated in this way.

[1]N. J. Horing, Phys. Rev. 186, 434 (1969).
[2]N. J. Horing, J. Phys. Soc. Jpn. Suppl. 21, 704 (1966).
[3]M. E. Rensink, Phys. Rev. 174, 744 (1968).
[4]M. L. Glasser, Phys. Rev. 180, 942 (1969).
[5]M. L. Glasser, Can. J. Phys. 48, 1941 (1970).
[6]J. Friedel, Nuovo Cimento Suppl. 2, 287 (1958).

[7]J. S. Langer and S. H. Vosko, J. Phys. Chem. Solids 12, 196 (1960).
[8]A. G. Eguiluz, Phys. Rev. B 23, 1542 (1981).
[9]N. J. Horing, Ann. Phys. (N.Y.) 54, 405 (1969).
[10]D. E. Beck, V. Celli, G. Lo Vecchio, and A. Magnaterra, Nuovo Cimento 68B, 230 (1970).
[11]J. W. Gadzuk, Solid State Commun. 5, 743 (1967); J. Phys. Chem. Solids 30, 2307 (1969).
[12]G. Gumbs and A. Griffin, J. Phys. F 12, 1185 (1982).
[13]G. Gumbs, Physica 111A, 343 (1982).
[14]G. Gumbs and D. J. W. Geldart, Physica 120A, 178 (1983).
[15]G. Gumbs, Phys. Rev. B 27, 7136 (1983).
[16]M. L. Glasser, in *Advances and Perspectives,* Vol. 2 of *Theoretical Chemistry,* edited by H. Eyring and D. Henderson (Academic, New York, 1976), p. 67.
[17]N. J. Horing and M. M. Yildiz, Ann. Phys. (N.Y.) 97, 216 (1976).
[18]T. Ando, A. B. Fowler, and F. Stern, Rev. Mod. Phys. 54, 437 (1982).
[19]I. S. Gradshteyn and I. M. Ryzhik, *Table of Integrals, Series and Products* (Academic, New York, 1965).
[20]In the quantum strong-field limit, we have

$$4\pi e^2\partial\bar{n}/\partial\mu=m^*\omega_p^2/2\mu\ ,$$

$$1-(4\pi e^2/m^*\omega_c)(\partial W/\partial\mu-\bar{n})=1-(\omega_p^2/\omega_c^2)(\hbar\omega_c/4\mu-1)\ ,$$

and

$$1-(\pi e^2\hbar^2/m^*)\partial^2\bar{n}/\partial\mu^2=1+(\hbar\omega_p/4\pi)^2\ .$$

The notation is defined in the text.
[21]N. J. Horing, R. W. Danz, and M. L. Glasser, Phys. Lett. 35A, 17 (1971).
[22]N. J. Horing, R. W. Danz, and M. L. Glasser, Phys. Rev. A 6, 2391 (1972).
[23]T. Yang, J. Trooster, T. Kachnowski, and N. Benczer-Koller, Hyperfine Interact. 10, 795 (1981).
[24]S. L. Ruby and G. K. Shenoy, in *Mössbauer Isomer Shifts,* edited by G. K. Shenoy and F. E. Wagner (North-Holland, New York, 1978), Chap. 9b.
[25]W. A. Harrison, *Electronic Structure and the Properties of Solids* (Freeman, San Francisco, 1980), p. 141.
[26]R. A. Krakowski and R. B. Miller, Nucl. Instrum. Methods 100, 93 (1972).
[27]J. Bainbridge, Nucl. Instrum. Methods 128, 531 (1975).
[28]G. P. Huffman, Nucl. Instrum. Methods 137, 267 (1976).